

## RESEARCH ARTICLE

10.1002/2013JD021294

## Key Points:

- Ozone seasonal maximum in tropical lower stratosphere
- Seasonal Maximum is Asymmetric with NH larger than SH
- Explained by timing of upwelling and mixing

## Correspondence to:

R. S. Stolarski,  
rstolar1@jhu.edu

## Citation:

Stolarski, R. S., D. W. Waugh, L. Wang, L. D. Oman, A. R. Douglass, and P. A. Newman (2014), Seasonal variation of ozone in the tropical lower stratosphere: Southern tropics are different from northern tropics, *J. Geophys. Res. Atmos.*, 119, 6196–6206, doi:10.1002/2013JD021294.

Received 2 DEC 2013

Accepted 23 APR 2014

Accepted article online 29 APR 2014

Published online 20 MAY 2014

# Seasonal variation of ozone in the tropical lower stratosphere: Southern tropics are different from northern tropics

Richard S. Stolarski<sup>1</sup>, Darryn W. Waugh<sup>1</sup>, Lei Wang<sup>1</sup>, Luke D. Oman<sup>2</sup>, Anne R. Douglass<sup>2</sup>, and Paul A. Newman<sup>2</sup>
<sup>1</sup>Department of Earth and Planetary Sciences, Johns Hopkins University, Baltimore, Maryland, USA, <sup>2</sup>Atmospheric Chemistry and Dynamics Branch, NASA Goddard Space Flight Center, Greenbelt, Maryland, USA

**Abstract** We examine the seasonal behavior of ozone by using measurements from various instruments including ozonesondes, Aura Microwave Limb Sounder, and Stratospheric Aerosol and Gas Experiment II. We find that the magnitude of the annual variation in ozone, as a percentage of the mean ozone, exhibits a maximum at or slightly above the tropical tropopause. The maximum is larger in the northern tropics than in the southern tropics, and the annual maximum of ozone in the southern tropics occurs 2 months later than that in the northern tropics, in contrast to usual assumption that the tropics can be treated as a horizontally homogeneous region. The seasonal cycles of ozone and other species in this part of the lower stratosphere result from a combination of the seasonal variation of the Brewer–Dobson circulation and the seasonal variation of tropical and midlatitude mixing. In the Northern Hemisphere, the impacts of upwelling and mixing between the tropics and midlatitudes on ozone are in phase and additive. In the Southern Hemisphere, they are not in phase. We apply a tropical leaky pipe model independently to each hemisphere to examine the relative roles of upwelling and mixing in the northern and southern tropical regions. Reasonable assumptions of the seasonal variation of upwelling and mixing yield a good description of the seasonal magnitude and phase in both the southern and northern tropics. The differences in the tracers and transport between the northern and southern tropical stratospheres suggest that the paradigm of well-mixed tropics needs to be revised to consider latitudinal variations within the tropics.

## 1. Introduction

The observations of tropical lower stratospheric ozone show variability on a range of time scales, including an annual cycle, interannual variations, and long-term trends [e.g., *World Meteorological Organization*, 2010]. Much of this temporal variability has been linked to variability in the tropical mean upwelling. For example, the large ozone annual cycle has been attributed to the annual cycle in the tropical mean upwelling [Randel *et al.*, 2007], and a negative trend deduced from Stratospheric Aerosol and Gas Experiment (SAGE) ozone data has been attributed to an increase in the upwelling bringing more ozone-poor air into the lower stratosphere [Randel and Thompson, 2011]. More recent studies have presented evidence that quasi-horizontal mixing with the extratropics plays an important role, at least for the annual cycle [e.g., Konopka *et al.*, 2009, 2010; Ploeger *et al.*, 2012; Abalos *et al.*, 2012, 2013a, 2013b]. While the above studies have all used ozone observations to estimate transport rates, they have all focused on variations in the tropic-wide average (of ozone and upwelling). Here we examine differences in the seasonal behavior of lower stratospheric ozone between the southern and northern tropics.

In section 2, we describe the data used in our analysis. Section 3 examines the annual cycle of the ozone in the southern and northern tropics as measured by several instruments, and the seasonal analysis of the two hemispheres is extended to the measurements of N<sub>2</sub>O and HCl. It is shown that the annual amplitude of the tracers is larger in the northern tropics than that in the southern tropics, and the annual maximum in the southern tropics occurs 2 months later than that in the northern tropics. The seasonal variations in transport that explain the tracer annual cycles are examined in section 4, including an analysis of annual upwelling in the southern and northern tropics. In section 5, we apply the tropical leaky pipe concept [Neu and Plumb, 1999] to show that the differences between the hemispheres in seasonal variations of trace constituents are consistent with reasonable assumptions concerning the seasonal cycle of upwelling and mixing. Finally, in

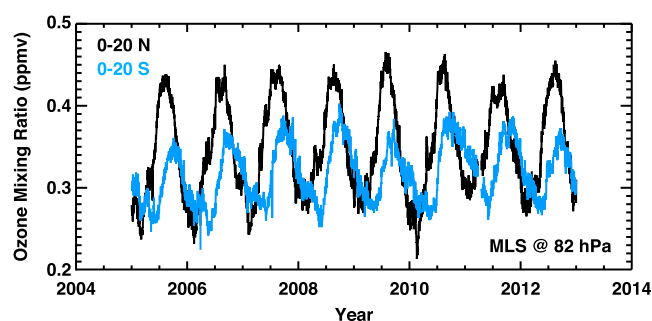


**Figure 1.** Time series of ozone measurements by Aura MLS at 82 hPa for zonal means averaged between 0–20°N (black curve) and 0–20°S (blue curve).

borne ozonesondes, Microwave Limb Sounder (MLS), and Stratospheric Aerosol and Gas Experiment II (SAGE II) satellite instruments.

Ozonesondes have been launched at numerous sites around the world for many decades. For the tropics, we rely on the ozonesonde stations of the SHADOZ (Southern Hemisphere Additional Ozonesonde) network [Thompson *et al.*, 2003a, 2003b, 2007]. The measurements in this network are made by electrochemical concentration cell sondes that are each calibrated before launch and subject to consistent procedures.

The MLS instrument was launched on the Aura satellite in 2004 and has made measurements from 2004 to 2013. Froidevaux *et al.* [2008] and Livesey *et al.* [2008] evaluate ozone data from MLS in detail. The version 3.3 data used here are described in the data quality document [Jet Propulsion Laboratory, 2011]. Ozone mixing ratios are retrieved from limb sounding measurements for pressure levels from 215 hPa up to 0.02 hPa with a vertical resolution of about 2.4 km. For our purpose of investigating tropical lower stratospheric ozone seasonal cycles, we focus on the retrievals between 200 hPa and 20 hPa with specific focus on 82 hPa and 68 hPa. For ozone, we focus on 82 hPa near the altitude of the peak of the tropical seasonal cycle shown in ozonesonde data in the next section. We also use MLS measurements of  $\text{N}_2\text{O}$  and HCl, which are potential tracers for atmospheric transport. The effective altitude resolution for HCl is about 3 km, while the effective resolution for  $\text{N}_2\text{O}$  is about 5.7 km.

The SAGE II instrument was launched in 1984 and measured ozone profiles using solar occultation from 1984 through 2005. We use version 6.2 [Wang *et al.*, 2002]. The SAGE occultation instrument gives 14 sunrise measurements per day at a single latitude and an additional 14 sunset measurements at a different latitude. The latitude for sunrise and sunset measurements progresses throughout the year to provide coverage from the south polar to north polar regions. Although seasonal coverage is sparse in the tropics, the length of the measurement record compensates for the sparse coverage, and we are able to successfully construct detailed seasonal behavior of ozone in the tropics from this 22 year data set. An important advantage of SAGE II measurements is their altitude resolution of approximately 1 km.

We also use the climatology of stratospheric and tropospheric ozone created by McPeters and Labow [2012] from a combination of MLS and ozonesonde measurements. The climatology is given in mixing ratio as a function of  $z^*$  levels in 1 km increments from the ground to 66 km. To obtain mixing ratios on a particular pressure surface, we converted  $z^*$  back to pressure and interpolated to the desired level.

### 3. Seasonal Variations in the Tropics

The time series of the daily zonal mean of ozone mixing ratio at 82 hPa measured by the Aura MLS instrument averaged over the 0–20°N and 0–20°S latitude bands shows that the annual cycles for the two regions are substantially different (Figure 1). In particular, the annual amplitude in the northern tropics (NT) is about double than that of the southern tropics (ST). The difference in amplitude between the NT and ST is almost entirely in the maximum values. The maximum ozone in the NT occurs in early August, whereas the ST maximum ozone is 1–2 months later. This phase shift of 2 months contrasts with the usual 6 month phase shift between the two hemispheres that is found at midlatitudes. The 2 month phase shift and the difference in the annual magnitude clearly illustrate that treating the tropics as a single horizontally homogeneous entity could lead to errors in interpretation.

section 6, we draw conclusions showing the importance of considering the northern and southern tropics separately when considering transport into and through the tropical lower stratosphere.

## 2. Data

We examine the seasonal variation of ozone and other species in the tropical lower stratosphere using data from three measurement systems: balloon-

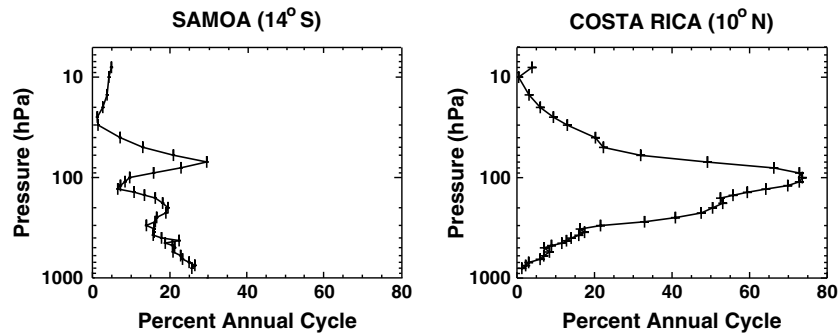


**Figure 2.** Vertical profiles of the percentage annual cycle of ozone for SHADOZ ozonesonde data at (left) Samoa (14°S) and (right) Costa Rica (10°N).

These differences in the tropical lower stratospheric ozone in the NT and ST are also found in ozonesonde data from the SHADOZ network. Figure 2 contrasts the seasonal cycle at Samoa (14°S) with that at Costa Rica (10°N). The measurements at Costa Rica show a maximum annual cycle, expressed as a percentage of the mean value, that is more than double than that of the maximum annual cycle at Samoa.

These examples illustrate the differences between the northern and southern tropical lower stratospheric seasonal cycles. To investigate these hemispheric differences in more detail, we examine the ozone seasonal behavior from three data sets: Aura MLS, SAGE II, and the *McPeters and Labow's* [2012] combined MLS-ozonesonde climatology.

Figure 3 shows the climatological monthly means at 82 hPa ozone from these three data sources. (82 hPa is a standard pressure level for MLS.) SAGE II measures number density at specific altitudes. To obtain ozone mixing ratios at 82 hPa from SAGE II, the temperatures reported with each SAGE II profile were used to convert number density versus altitude to mixing ratio at 82 hPa. Each of these data sources shows differences between the NT and ST seasonal variations. In the NT (solid curves), the peak ozone values of between 0.42 and 0.44 ppmv occur in the late summer, while minimum values ranging from 0.2 to nearly 0.3 ppmv occur in winter. In the ST (dashed curves), the maximum values are again nearly the same in all the three data sources (at about 0.35 ppmv), while the minima vary from less than 0.22 to about 0.28 ppmv. In both the NT and ST, the SAGE II ozone decreases more quickly after it reaches its maximum value than ozone from the other data sources.

To quantify the seasonal cycle from each data source, we fit the seasonal variation to annual and semiannual sines and cosines at each latitude and altitude of the measurements. From these, we determine the

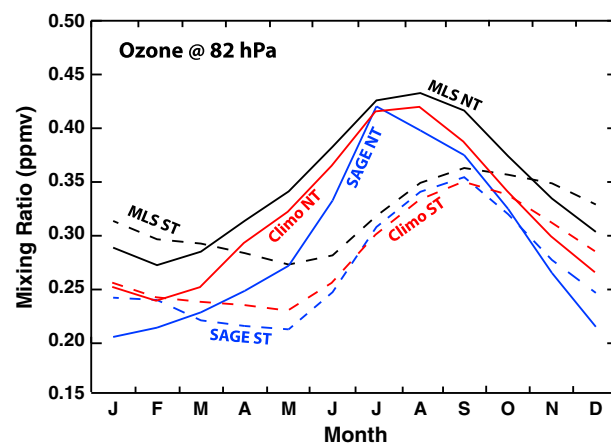


**Figure 3.** Climatological mean annual cycle of ozone at 82 hPa for the northern tropics (NT; 0–20°N) and southern tropics (ST; 0–20°S) from the measurements by Aura MLS (black curves), SAGE II (blue), and the *McPeters/Labow* climatology (red). Solid curves are northern tropics and dashed curves are southern tropics.

magnitude of the annual component, see Figure 4. Each also shows a maximum in the lower tropical stratosphere that is more pronounced in the northern tropics than that in the southern tropics. The maximum, shifted into the Northern Hemisphere, can also be seen in the Halogen Occultation Experiment data [see *Randel et al.*, 2007, Figure 4].

There are significant differences in the detailed structure of the maxima obtained from the three data sets. MLS shows a double maximum in the magnitude of the annual term in the seasonal cycle in the northern tropics. The peaks are at the retrieval levels of 68 hPa (~30%) and 100 hPa (~35%) with a lesser magnitude of the annual term at the 82 hPa retrieval level. This behavior of the seasonal cycle does not

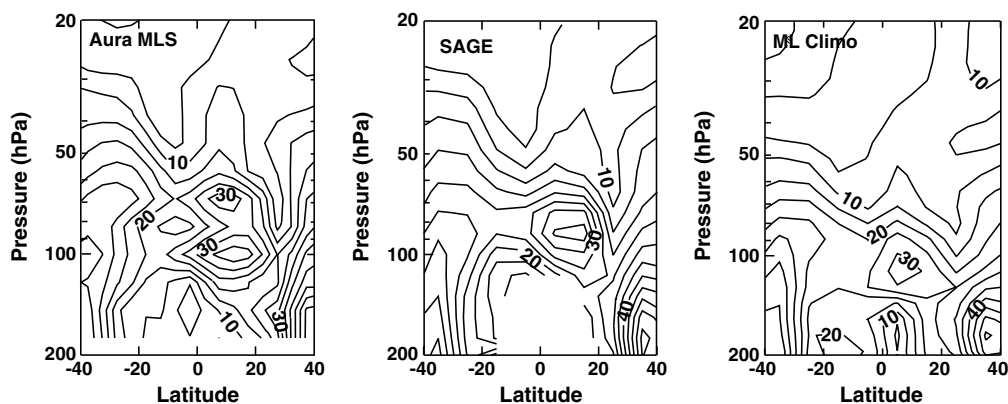


**Figure 4.** Latitude-altitude dependence of the magnitude of the annual cycle in ozone, in percent of the mean value, for (a) 8 years of Aura MLS data, (b) 21 years of SAGE II data, and (c) *McPeters and Labow* [2012] climatology.

appear to be caused by the observed oscillations in the ozone profiles retrieved by version 3.3 in the tropical lower stratosphere [*Livesey et al.*, 2013], as similar behavior is observed using the earlier MLS version 2.2 retrieval. SAGE II shows a single peak in the Northern Hemisphere (NH) near 80 hPa (~35%). The *McPeters/Labow* climatology combines MLS and sonde data in this region and shows a single NH peak at about 100 hPa (~30%).

Rather than further investigation of the differences among data sets that may be due to vertical resolution, sampling, or length of record, in the following sections, we examine the robust features of the observed seasonal variations of ozone. These are the following: (1) both southern and northern tropics show a maximum percentage seasonal cycle in the lower stratosphere, (2) the northern tropics' annual amplitude is larger than that for the southern tropics' annual amplitude, and (3) the maximum in the northern tropics occurs 2 months earlier than that for the southern tropics.

We also examined the MLS observations of the long-lived tracers  $\text{N}_2\text{O}$  and  $\text{HCl}$  at 68 hPa (these species are not reported by MLS at 82 hPa).  $\text{HCl}$  is a long-lived reservoir for chlorine that is similar to ozone; in that, it is formed in the middle to upper stratosphere and then transported to the rest of the stratosphere. Its seasonal behavior in the tropics is similar to that observed for ozone, as shown in Figure 5a.  $\text{N}_2\text{O}$  is the opposite to  $\text{O}_3$  and  $\text{HCl}$ ; in that, it is released in the troposphere and transported up to the stratosphere, where it is destroyed by photolysis and chemical reaction. Its seasonal behavior is the opposite of that for ozone and  $\text{HCl}$ , as shown in Figure 5b. The magnitude of the seasonal cycle of  $\text{N}_2\text{O}$  is much smaller than that for either  $\text{O}_3$  or  $\text{HCl}$ , because the gradients, both vertical and horizontal, on which the transport processes are operating are much

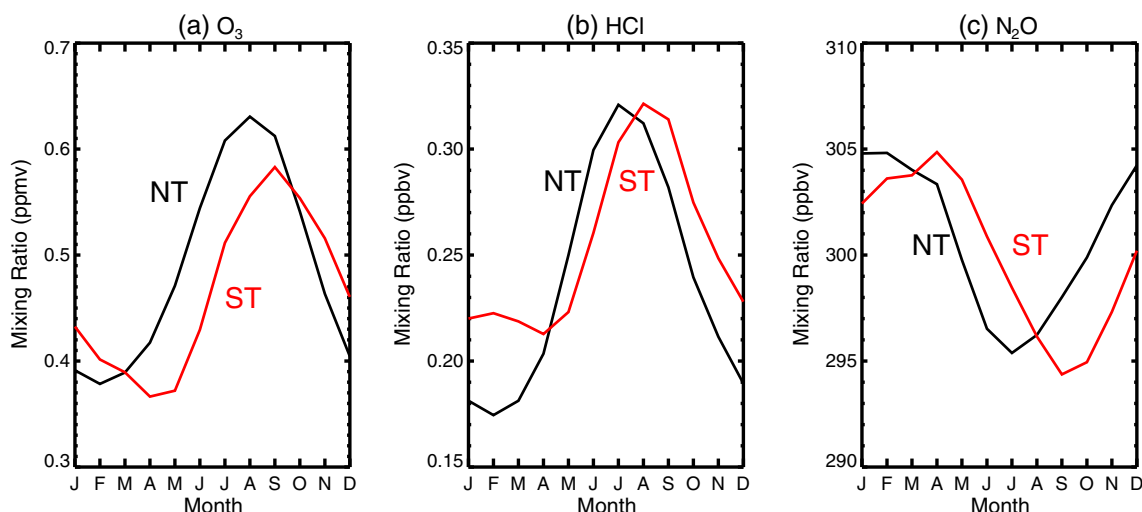


**Figure 5.** Mean seasonal cycle for (a)  $\text{O}_3$ , (b)  $\text{HCl}$ , and (c)  $\text{N}_2\text{O}$  at 68 hPa in the NT and ST as measured by Aura MLS.

smaller for  $\text{N}_2\text{O}$ . Note that the difference between the NT and ST for  $\text{N}_2\text{O}$  occurs primarily in the minimum value, whereas the difference for ozone occurs primarily in the maximum value. The ozone maximum is occurring in the same season as the  $\text{N}_2\text{O}$  minimum, consistent with the gradients for  $\text{N}_2\text{O}$  being in the opposite direction as those for ozone. The hemispheric difference for HCl also occurs primarily in the minimum values. It is not clear how to explain this observation.

#### 4. Seasonal Variations in Transport

We assert that the seasonal behavior of ozone, HCl, and  $\text{N}_2\text{O}$  in the tropical lower stratosphere is due to the seasonality of transport operating on tracer gradients. Transport in the tropical lower stratosphere is primarily due to a combination of vertical advection (by the residual circulation) and mixing between the tropics and extratropics [e.g., *Hall and Waugh, 1997; Plumb, 2002*]. The phase and relative amplitude of the tracer annual cycles will depend on the seasonality of the upwelling and mixing between the tropics and extratropics as well as the vertical and horizontal tracer gradients.

In the analysis, here we focus on the variations in the concentration of ozone and other tracers averaged within the geographical tropics (i.e., averaged between fixed latitudes), as such averaging is most commonly done in the analysis of seasonal and longer-term variations in tropical ozone. It may be more appropriate to define the tropics with respect to subtropical mixing barriers (i.e., minima in horizontal mixing). There is a seasonal cycle in the latitude of these barriers [e.g., *Haynes and Shuckburgh, 2000*] (see Figure 8). The mixing with respect to fixed latitudes discussed below could then be viewed as a combination of physical mixing across a mixing barrier and the movement of barrier into and out of the geographical tropics.

The seasonal variations (and differences between the ST and NT) are similar for ozone and HCl and nearly the opposite for  $\text{N}_2\text{O}$ . This is because of the differences in the spatial gradients of the tracers. Figure 6 shows the mean vertical distribution of each of the three species in the tropics and their latitudinal distribution at 68 hPa. The vertical gradients in the tropics for ozone and HCl are positive upward, while that for  $\text{N}_2\text{O}$  is negative upward. The latitudinal gradients for ozone and HCl are positive away from the tropics, while those for  $\text{N}_2\text{O}$  is negative away from the tropics.

The transport-induced seasonal variations in the tracers could be due to seasonal variations in the upwelling of (ozone-poor, HCl-poor, and  $\text{N}_2\text{O}$ -rich) air from below, the mixing of (ozone-rich, HCl-rich, and  $\text{N}_2\text{O}$ -poor) air into the tropics from midlatitudes, or both processes. We first consider the variations in the upwelling from below by the residual vertical velocity,  $w^*$ . A large annual cycle in tropical  $w^*$ , averaged over the tropics, has been reported [*Rosenlof, 1995; Randel et al., 2007, 2008; Yang et al., 2008; Seviour et al., 2012*], but there has been less examination of the latitudinal variations within the tropics. These previous studies have also shown differences among  $w^*$  obtained from different meteorological reanalysis products, so we examine  $w^*$  from three reanalyses: ERA-40 [*Uppala et al., 2005*], ERA-Interim [*Seviour et al., 2012*], and Modern-Era Retrospective Analysis for Research and Applications (MERRA) [*Rienecker et al., 2011*].

Figure 7 shows the seasonal variation of 100 hPa  $w^*$  averaged over ST (Figure 7a) and NT (Figure 7b) for the three reanalyses. There are some differences in detail among the different reanalyses, but all three indicate that the annual variation of ST  $w^*$  differs from that in the NT. There is a clear annual cycle in ST  $w^*$  with a maximum around December–February and minimum around June–August, whereas the seasonality of  $w^*$  in the NT has a much smaller seasonal dependence with a peak in April–May in all reanalyses and a second peak in November for the ERA reanalyses.

The comparison of the annual cycles of  $w^*$  with that of the tracers shows that seasonal variations in  $w^*$  alone cannot explain the hemispheric differences in the seasonal variations of tracers. The amplitude of seasonal cycle in  $w^*$  is much larger in the ST than in the NT, but the opposite is found for ozone. Furthermore, while the  $w^*$  and the trace gases have similar seasonal variations in the Southern Hemisphere, the seasonal variations of  $w^*$  and trace gases are different in the NH. This suggests that the seasonal variations in the mixing between the tropics and extratropics play a major role in causing the seasonal variations in the tracers.

To examine the role of mixing, we revisit the Aura MLS data. The excellent spatial coverage obtained by MLS for several species makes it possible to examine the time-space variations in more detail. Figure 8a shows the time-latitude variation of the climatological zonal-mean ozone measured by MLS at 82 hPa. The figure was constructed from 8 years of monthly mean ozone amounts in  $2^\circ$  latitude bands, and the April to September

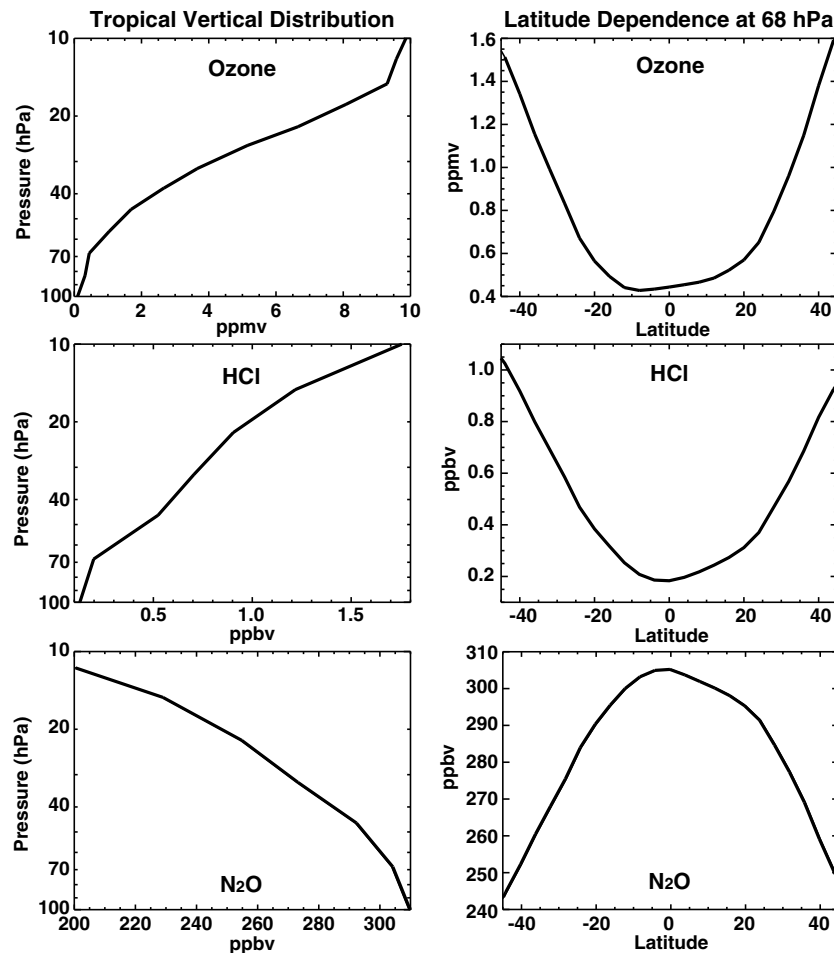


**Figure 6.** (first column) Mean vertical distribution of ozone, HCl, and N<sub>2</sub>O in the tropics (8°S–8°N) as measured by MLS on Aura. (second column) Mean latitudinal distribution of ozone, HCl, and N<sub>2</sub>O at 68 hPa as measured by MLS on Aura.

climatology are shown twice. The primary feature of this diagram is the closely packed contours in the midlatitudes that move back and forth with season. This corresponds to the tropical region of the lower stratosphere moving to the north during northern summer and to the south during southern summer. These contours indicate a strong gradient that gives way to a much weaker gradient in the tropics. Although the illustration of quasi-horizontal mixing would be more physical if done on an isentropic level, we have chosen to show the data on a pressure level that is the natural coordinate for the MLS retrieval.

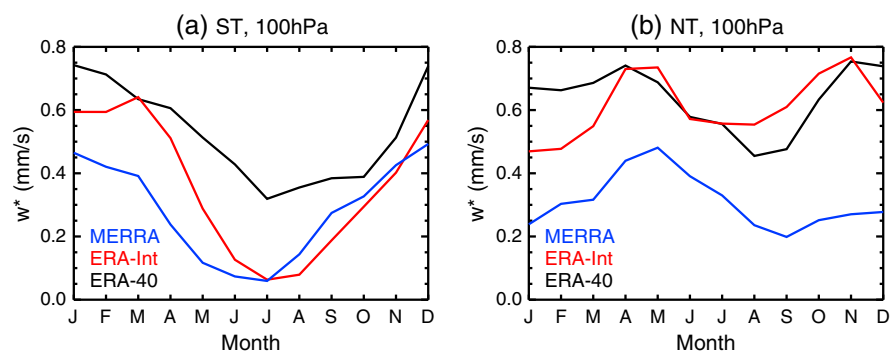


**Figure 7.** Mean annual cycle for 100 hPa  $w^*$  in (a) ST and (b) NT from MERRA (blue), ERA-Interim (red), and ERA-40 (black) reanalyses.



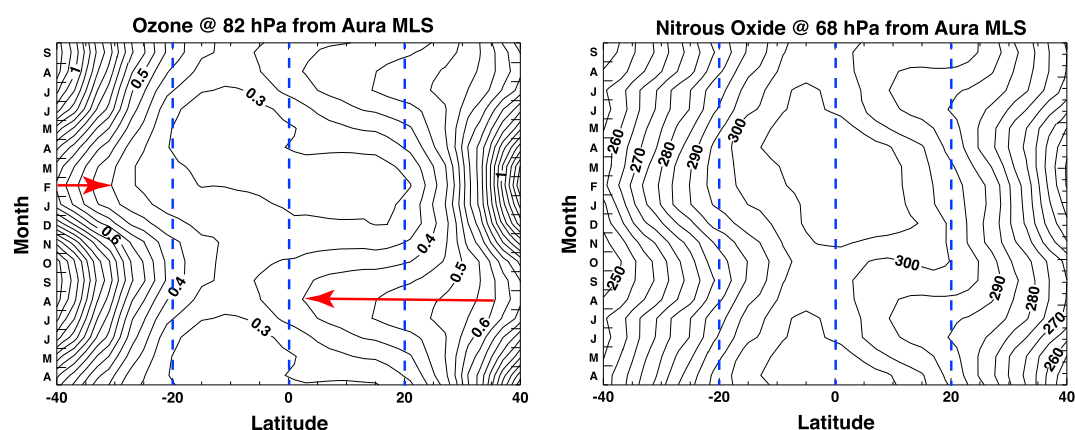


**Figure 8.** Latitude/time plot of mixing ratio of (a) 82 hPa ozone and (b) 68 hPa  $\text{N}_2\text{O}$  from the measurements on Aura MLS. Ozone mixing ratios are in parts per million by volume, and nitrous oxide mixing ratios are in parts per billion by volume. Results are from a monthly mean climatology in  $2^\circ$  latitude bands repeated with 18 months shown from April through September. Red arrows are drawn from the 0.6 contour to the 0.4 contour in the summer of the northern and southern tropics to emphasize the apparent strong mixing into the northern tropics. Blue dashed lines are drawn at  $20^\circ\text{S}$ , equator, and  $20^\circ\text{N}$  to show the two tropical regions considered in the analysis.

An important secondary feature in Figure 8a is the apparent spreading of the contours during northern summer into the tropics. The red arrows in Figure 8a are drawn from the 0.6 ppmv contour to the 0.4 ppmv contour during northern and southern summers. The spread between these contours is many times larger in the northern summer than that in the southern summer and is consistent with the larger transport of ozone from the high-ozone midlatitudes into the low-ozone tropics during northern summer.

The MLS  $\text{N}_2\text{O}$  data (Figure 8b) show the same spreading of contours into the tropics from the Northern Hemisphere during the northern summer with little spreading from the Southern Hemisphere during southern summer. The gradient for  $\text{N}_2\text{O}$  is reversed from that of the ozone, and the transport of air into the tropics brings lower mixing ratio characteristic of midlatitudes. The  $\text{N}_2\text{O}$  measurements are shown at 68 hPa, because the retrieved MLS profiles of  $\text{N}_2\text{O}$  are reported at every other level as a trade-off between vertical resolution and precision of retrieval.

The seasonal variations in gradients of ozone and  $\text{N}_2\text{O}$  are consistent with previous studies that indicate that the mixing into the northern tropics is strongest during the northern summer [see e.g., Haynes and Shuckburgh, 2000; Konopka et al., 2009]. Furthermore, the longitudinal dependence of the seasonal variations in the NT are consistent with the mixing being associated with the Asian and North American Monsoons [e.g., Shuckburgh et al., 2009].

Taken together, the above analysis suggests that the differences in the seasonal variations in lower stratospheric ozone between the northern and southern tropics are due to interhemispheric differences in both the magnitude and phase of seasonal variations in the upwelling and mixing. The annual cycle in  $w^*$  within the ST is much larger than in the NT, whereas there is a larger seasonal variation in the mixing in the NT. Thus, seasonality in upwelling plays a larger role in the tracer seasonality in the ST, whereas seasonality in mixing is more important to tracer seasonality in the NT. The relative phase of the seasonal variations in upwelling and mixing is also important. In the NT, the cycles in upwelling and mixing are roughly 6 months out of phase. Minimum upwelling and maximum mixing both occur during June-July-August with both contributing to the ozone maximum observed during this season. Hence, these processes act together, resulting in a large annual cycle in tracers. In contrast, in the ST, the upwelling and mixing are roughly in phase, and these processes have opposing effects on the tracers resulting in partial cancellation and weaker seasonal variations of tracers in the ST. Thus, the impacts of upwelling and mixing are effectively in-phase in the NT and out-of-phase in the ST.

## 5. Tropical Leaky Pipe Model

The above analysis of observations indicates that the different annual cycles of lower stratospheric ozone (and other trace gases) in the ST and NT are due to the differences in amplitude and phase of seasonal variations in

the tropical upwelling and mixing with midlatitudes. To test this hypothesis, we perform simulations using a tropical leaky pipe (TLP) model [e.g., Plumb, 1996; Neu and Plumb, 1999; Hall and Waugh, 1997].

We consider the extreme case where there is no flow/exchange across the equator, and the two hemispheres are isolated from each other and can each be modeled as a TLP. In this simple model, each hemisphere consists of two coupled 1-D regions of vertical motion, one representing the tropics (upwelling) and the other a horizontally well-mixed midlatitudes (downwelling). The regions are coupled by the tropical outflow consistent with the divergent upwelling and by independently specified two-way tropical-midlatitude mixing. Again, we are considering the variations in tracers averaged within the geographical tropics, and the tropical-midlatitude mixing could be a combination of physical mixing across a mixing barrier and the movement of barrier into and out of the geographical tropics.

For this model, the continuity equations for the tracer concentrations in the tropics and extratropics ( $C_T$  and  $C_E$ ) are

$$\frac{\partial C_T}{\partial t} + W \frac{\partial C_T}{\partial z} - K_T e^{z/H} \frac{\partial}{\partial z} \left( e^{-z/H} \frac{\partial C_T}{\partial z} \right) = -\mu(C_T - C_E) + S_T \quad (1)$$

$$\frac{\partial C_E}{\partial t} - \alpha W \frac{\partial C_E}{\partial z} - K_E e^{z/H} \frac{\partial}{\partial z} \left( e^{-z/H} \frac{\partial C_E}{\partial z} \right) = (\lambda + \alpha\mu)(C_T - C_E) + S_E \quad (2)$$

where  $W$  is the vertical velocity in the tropics,  $K_T$  is the vertical diffusivity in the tropics,  $K_E$  is the vertical diffusivity in the extratropics,  $\mu$  is the mixing rate between the tropics and extratropics ( $\mu = 1/\tau$ , where  $\tau$  is the mixing time between the tropics and extratropics),  $H$  is the scale height,  $S$  is the tracer source,  $\alpha$  is the ratio of tropics to midlatitudes (0.5 in our calculations), and

$$\lambda = \alpha e^{z/H} \frac{\partial}{\partial z} \left( e^{-z/H} W \right)$$

is the rate of net entrainment from tropics into midlatitudes. The solutions for this two-region model are equivalent to the solutions of the three-region TLP considered in previous studies [e.g., Plumb, 1996; Neu and Plumb, 1999; Hall and Waugh, 1997] when the northern and southern midlatitudes are assumed to be identical.

This TLP model has three main parameters: tropical upwelling  $W$ , the tropical-midlatitude mixing rate  $\mu$  (with  $\mu = 0$  corresponding to complete the isolation between tropics and midlatitudes, and  $\mu = \infty$  corresponding to no isolation), and vertical diffusivities ( $K_T$  and  $K_E$ ). In the numerical simulations performed here, all the parameters are assumed to be independent of height. The diffusivities are constant with time ( $K_T = 0.01 \text{ m}^2/\text{s}$  and  $K_E = 0.5 \text{ m}^2/\text{s}$ ), but  $W$  and  $\mu$  vary with annual cycles:

$$\begin{aligned} W &= W_0(1 + A_w \cos(2\pi t - \phi_w)) \\ \mu &= \mu_0(1 + A_\mu \cos(2\pi t - \phi_\mu)) \end{aligned}$$

In all simulations, the mean tropical upwelling rate is  $W_0 = 0.3 \text{ mm/s}$ , whereas the mean mixing rate is  $\mu_0 = 1.01/\text{yr}$ . The mean values are the same or similar to the values used in previous studies of tropical lower stratospheric transport [Neu and Plumb, 1999; Hall and Waugh, 2000].

We focus here on the TLP simulations of the mean age of stratospheric air,  $\Gamma$  [e.g., Waugh and Hall, 2002]. The symbol  $\Gamma$  is the mean transit time from the tropopause and can be simulated in the TLP model by setting  $S_T = S_E = 1 \text{ yr/yr}$  and  $C_T = C_E = 0$  at  $Z = 0$  [Neu and Plumb, 1999]. We consider  $\Gamma$  because it is determined solely by transport, and the sign of the vertical and horizontal gradients of  $\Gamma$  are the same as for ozone (i.e., both  $\Gamma$  and ozone increase with altitude in the tropical lower stratosphere, and in the lower stratosphere, both are larger in middle latitude than the tropics).

We first consider the cases where only one of  $W$  or  $\mu$  varies seasonally. In both cases, the TLP model produces an annual cycle in  $\Gamma$ . For the case with an annual cycle in  $W$  but constant  $\mu$ , the peak in tropical lower stratosphere  $\Gamma$  occurs around 2 months after the minimum in  $W$ , which corresponds to the maximum in vertical advection time,  $1/W$ . For varying  $\mu$  and constant  $W$ , the peak in  $\Gamma$  occurs about 1 month after the maximum in the mixing rate  $\mu$ .



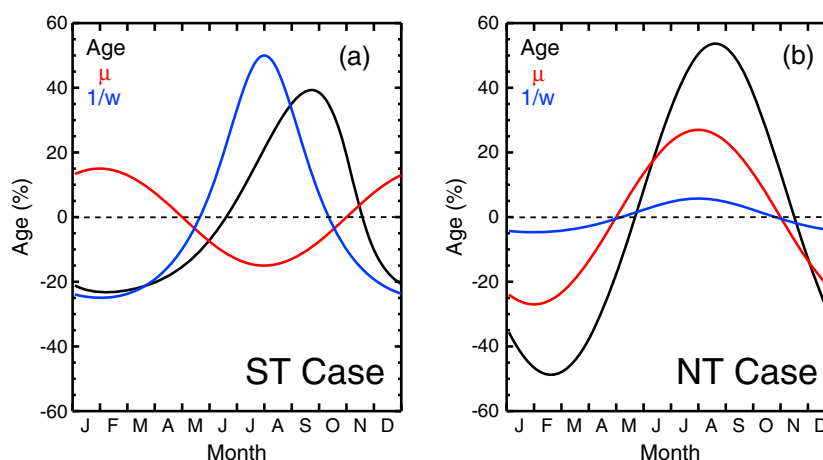


**Figure 9.** Seasonal variation of mean age at  $z=2$  km above the tropical tropopause from TLP model for cases with (a) strong annual cycle in  $W$  and modest annual cycle in mixing rate, with both minimum in July ( $A_W=0.6$ ,  $\phi_W=0$ ,  $A_\mu=0.5$ , and  $\phi_\mu=0$ ), or (b) weak annual cycle in  $W$  with minimum in July and large annual cycle in mixing time with minimum in January ( $A_W=0.25$ ,  $\phi_W=0$ ,  $A_\mu=0.9$ , and  $\phi_\mu=\pi$  years). The mixing rate  $1/w$  and  $\mu$  are rescaled for display purpose. Figure 9a is the representative of the southern tropics, while Figure 9b is the representative of the northern tropics.

An extensive series of simulations has been performed, where both  $W$  and  $\mu$  vary seasonally. These show that the amplitude and phase of the annual cycles in  $\Gamma$  depend not only on  $A_W$  and  $A_\mu$ , but also on the relative phase of these cycles (not shown). For example, for given  $A_W$  and  $A_\mu$ , the maximum amplitude of the annual cycle in  $\Gamma$  occurs when the minimum in  $W$  and the maximum in  $\mu$  occur at the same time. The phase of the  $\Gamma$  cycle also depends on the relative timing of the  $W$  and  $\mu$  cycles, but the dependence is weak when there is a large  $W$  cycle. To understand the seasonality of tracers, it is therefore important to consider both the amplitude and phase of variations in the transport parameters (processes).

We consider now the TLP simulations, where the amplitude and phase of  $W$  and  $\mu$  mimic the observed (or inferred) variations. The analysis in previous sections shows that the minimum in  $W$  occurs around July in both the southern and northern tropics, but the amplitude in the southern tropics is much larger (i.e.,  $A_W \sim 0.6$  in southern tropics but  $A_W \sim 0.25$  in northern tropics.). The above analysis also indicates that the tropical-midlatitude mixing in the lower stratosphere also varies seasonally, with maximum mixing (i.e., maximum in  $\mu$ ) during summer and largest seasonality in the Northern Hemisphere).

TLP simulations have been performed where the parameters have the above seasonal variations. For example, Figure 9a shows the simulated  $\Gamma$  for a case mimicking the Southern Hemisphere: the annual cycle in  $W$  has a large amplitude ( $A_W=0.6$ ) with minimum in July, while the annual cycle in  $\mu$  has a moderate amplitude ( $A_\mu=0.5$ ) also with minimum in July. Figure 9b shows a case representative of the NH, with a weak amplitude in  $W$  ( $A_W=0.25$ ) with minimum in July but large amplitude in  $\mu$  ( $A_\mu=0.9$ ) that has minimum in January. The resulting annual cycles in  $\Gamma$  resemble the observed ozone annual cycles in southern and northern tropics, respectively; i.e., there is a larger amplitude in Figure 9b that occurs earlier than in Figure 9a (August compared to September).

These examples illustrate that the key features of the observed seasonality of trace gases in the tropical lower stratosphere are reproduced in the TLP model when the above hypothesized seasonal variations in the upwelling and mixing (a large annual cycle in upwelling and moderate cycle in mixing in ST that are in phase and moderate cycle in upwelling and large mixing cycle that are out of phase in NT) are used. Hence, providing support for this hypothesis. Given the simplistic nature of the TLP model, we do not attempt to determine the parameters to fit the observed ozone seasonal variations.

## 6. Summary and Conclusions

We have shown that the seasonal cycle of ozone is stronger in the northern tropical lower stratosphere than that in the southern tropical lower stratosphere and that the seasonal cycle maximum of ozone in the

southern tropics is about 2 months delayed from the northern tropics' maximum. This hemispheric asymmetry in the ozone seasonal cycle is present in the data from ozonesondes as well as from satellite measurements by SAGE II and Aura MLS. Further, a contrast between the seasonal behavior in the northern and southern tropics also occurs in the Aura MLS measurements of  $\text{N}_2\text{O}$  and HCl.

These differences in the seasonal variations between hemispheres imply hemispheric differences in the transport in the tropical lower stratosphere. The analysis of the residual vertical velocity  $w^*$  from reanalyses and tracer subtropical gradients together with simulations using a simple tropical leaky pipe (TLP) model suggests that there are hemispheric differences in the amplitude and phase of the annual cycles in the tropical upwelling and in the horizontal mixing with the extratropics. Specifically, there is a large annual cycle in upwelling and moderate cycles in mixing in the southern tropics that are in phase, whereas there is a moderate cycle in the upwelling and large mixing cycles that are out of phase in the northern tropics.

The above differences in the transport between the northern and southern tropical stratosphere suggests that the paradigm of well-mixed tropics (both for composition and transport properties) needs to be revised to consider latitudinal variations within the tropics. This new view has the potential to not only change our understanding of the balance between upwelling and quasi-horizontal mixing in the tropical lower stratosphere but also modify our understanding of how this transport, and composition, will respond to increases in greenhouse gases and other changes in climate.

It also suggests the need for a more detailed evaluation of the tropical composition and transport in chemistry-climate models. A preliminary look at the *Stratospheric Processes and their Role in Climate Chemistry-Climate Model Validation* [2010] models shows that the models generally reproduce the characteristics of the seasonal cycle, including the contrast between the northern and southern tropics. This suggests that the models include the key processes that cause the annual cycle in ozone (and differences between the northern and southern tropics). However, there is a large spread in the amplitude of the annual cycles among the models, indicating significant differences in the model transport. The analysis of these differences may provide a critical evaluation of how well the models simulate tropical lower stratospheric transport and composition.

#### Acknowledgments

We thank Stacey Frith for converting the SAGE data from number density versus altitude to mixing ratio versus pressure. We also thank three anonymous reviewers for their helpful comments on the manuscript.

#### References

- Abalos, M., W. J. Randel, and E. Serrano (2012), Variability in upwelling across the tropical tropopause and correlations with tracers in the lower stratosphere, *Atmos. Chem. Phys.*, **12**, 11,505–11,517, doi:10.5194/acp-12-11505-2012.
- Abalos, M., W. J. Randel, D. E. Kinnison, and E. Serrano (2013a), Quantifying tracer transport in the tropical lower stratosphere using WACCM, *Atmos. Chem. Phys.*, **13**, doi:10.5194/acp-13-10591-2013.
- Abalos, M., F. Ploeger, P. Konopka, W. J. Randel, and E. Serrano (2013b), Ozone seasonality above the tropical tropopause: Reconciling the Eulerian and Lagrangian perspectives of transport processes, *Atmos. Chem. Phys.*, **13**(21), 10,787–10,794, doi:10.5194/acp-13-10787-2013.
- Froidevaux, L., et al. (2008), Validation of Aura Microwave Limb Sounder stratospheric ozone measurements, *J. Geophys. Res.*, **113**, D15S20, doi:10.1029/2007JD008771.
- Hall, T. M., and D. W. Waugh (1997), Tracer transport in the tropical stratosphere due to vertical diffusion and horizontal mixing, *Geophys. Res. Lett.*, **24**, 1383–1387, doi:10.1029/97GL01289.
- Hall, T. M., and D. W. Waugh (2000), Stratospheric residence time and its relationship to mean age, *J. Geophys. Res.*, **105**, 6773–6782, doi:10.1029/1999JD901096.
- Haynes, P., and E. Shuckburgh (2000), Effective diffusivity as a diagnostic of atmospheric transport: 1. Stratosphere, *J. Geophys. Res.*, **105**, 22,777–22,794, doi:10.1029/2000JD900093.
- Jet Propulsion Laboratory (2011), Earth Observing System (EOS) Aura Microwave Limb Sounder (MLS) Version 3.3 Level 2 data quality and description document, *Rep. JPL D-33509*, Jet Propul. Lab., Pasadena, Calif.
- Konopka, P., J.-U. Grooß, F. Ploeger, and R. Müller (2009), R.: Annual cycle of horizontal in-mixing into the lower tropical stratosphere, *J. Geophys. Res.*, **114**, D19111, doi:10.1029/2009JD011955.
- Konopka, P., J.-U. Grooß, G. Günther, F. Ploeger, R. Pommrich, R. Müller, and N. Livesey (2010), N.: Annual cycle of ozone at and above the tropical tropopause: Observations versus simulations with the Chemical Lagrangian Model of the Stratosphere (CLaMS), *Atmos. Chem. Phys.*, **10**, 121–132, doi:10.5194/acp-10-121-2010.
- Livesey, N. J., et al. (2008), Validation of Aura Microwave Limb Sounder  $\text{O}_3$  and CO observations in the upper troposphere and lower stratosphere, *J. Geophys. Res.*, **113**, D15S02, doi:10.1029/2007JD008805.
- Livesey, N. J., et al. (2013), Earth Observing System (EOS) Aura Microwave Limb Sounder (MLS) Version 3.3 and 3.4 Level 2 data quality and description document, *JPL D-33509*, Pasadena, Calif.
- McPeters, R. D., and G. J. Labow (2012), Climatology 2011: An MLS and sonde derived ozone climatology for satellite retrieval algorithms, *J. Geophys. Res.*, **117**, D10303, doi:10.1029/2011JD017006.
- Neu, J. L., and R. A. Plumb (1999), Age of air in a "leaky pipe" model of stratospheric transport, *J. Geophys. Res.*, **104**, 19,243–19,255, doi:10.1029/1999JD900251.
- Ploeger, F., P. Konopka, R. Müller, S. Fueglistaler, T. Schmidt, J. C. Manners, J.-U. Grooß, G. Günther, P. M. Forster, and M. Riese (2012), Horizontal transport affecting trace gas seasonality in the Tropical Tropopause Layer (TTL), *J. Geophys. Res.*, **117**, D09303, doi:10.1029/2011JD017267.
- Plumb, R. A. (1996), A "tropical pipe" model of stratospheric transport, *J. Geophys. Res.*, **101**, 3957–3972, doi:10.1029/95JD03002.
- Plumb, R. A. (2002), Stratospheric transport, *J. Met. Soc. Jpn.*, **80**(4B), 793–809.

- Randel, W. J., and A. M. Thompson (2011), Interannual variability and trends in tropical ozone derived from SAGE II satellite data and SHADOZ ozonesondes, *J. Geophys. Res.*, **116**, D07303, doi:10.1029/2010JD015195.
- Randel, W. J., M. Park, F. Wu, and N. Livesey (2007), A large annual cycle in ozone above the tropical tropopause linked to the Brewer-Dobson circulation, *J. Atmos. Sci.*, **64**(12), 4479–4488, doi:10.1175/2007JAS2409.1.
- Randel, W. J., R. Garcia, and F. Wu (2008), Dynamical balances and tropical stratospheric upwelling, *J. Atmos. Sci.*, **65**, 3584–3595.
- Rienecker, M. M., et al. (2011), MERRA: NASA's Modern-Era Retrospective Analysis for Research and Applications, *J. Clim.*, **24**(14), 3624–3648, doi:10.1175/JCLI-D-11-00015.1.
- Rosenlof, K. H. (1995), Seasonal cycle of the residual mean meridional circulation in the stratosphere, *J. Geophys. Res.*, **100**, 5173–5191, doi:10.1029/94JD03122.
- Seviour, W. J. M., N. Butchart, and S. C. Hardiman (2012), The Brewer–Dobson circulation inferred from ERA-Interim, *Q. J. R. Meteorol. Soc.*, **138**, 878–888, doi:10.1002/qj.966.
- Shuckburgh, E., F. d'Ovidio, and B. Legras (2009), Local mixing events in the upper troposphere and lower stratosphere. Part II: Seasonal and interannual variability, *J. Atmos. Sci.*, **66**, 3695–3706.
- Stratospheric Processes and their Role in Climate Chemistry-Climate Model Validation (2010), SPARC CCMVal Report on the Evaluation of Chemistry-Climate Models, *Rep. 5, WCRP-132, WMO/TD-No. 1526*, edited by V. Eyring, T. G. Shepherd, and D. W. Waugh, SPARC, Toronto, Canada. [Available at <http://www.atmosp.physics.utoronto.ca/SPARC/>]
- Thompson, A. M., et al. (2003a), Southern Hemisphere Additional Ozonesondes (SHADOZ) 1998–2000 tropical ozone climatology 1. Comparison with Total Ozone Mapping Spectrometer (TOMS) and ground-based measurements, *J. Geophys. Res.*, **108**(D2), 8238, doi:10.1029/2001JD000967.
- Thompson, A. M., et al. (2003b), Southern Hemisphere Additional Ozonesondes (SHADOZ) 1998–2000 tropical ozone climatology 2. Tropospheric variability and the zonal wave-one, *J. Geophys. Res.*, **108**(D2), 8241, doi:10.1029/2002JD002241.
- Thompson, A. M., J. C. Witte, H. G. J. Smit, S. J. Oltmans, B. J. Johnson, V. W. J. H. Kirchhoff, and F. J. Schmidlin (2007), Southern Hemisphere Additional Ozonesondes (SHADOZ) 1998–2004 tropical ozone climatology: 3. Instrumentation, station-to-station variability, and evaluation with simulated flight profiles, *J. Geophys. Res.*, **112**, D03304, doi:10.1029/2005JD007042.
- Uppala, S. M., et al. (2005), The ERA-40 re-analysis, *Q. J. R. Meteorol. Soc.*, **131**, 2961–3012.
- Wang, H. J., D. M. Cunnold, L. W. Thomason, J. M. Zawodny, and G. E. Bodeker (2002), Assessment of SAGE version 6.1 ozone data quality, *J. Geophys. Res.*, **107**(D23), 4691, doi:10.1029/2002JD002418.
- Waugh, D. W., and T. M. Hall (2002), Age of stratospheric air: Theory, observations, and models, *Rev. Geophys.*, **40**(4), 1010, doi:10.1029/2000RG000101.
- World Meteorological Organization (2010), Scientific Assessment of Ozone Depletion: 2010, WMO Global Ozone Research and Monitoring Project-Report No. 52, Geneva, Switzerland.
- Yang, Q., Q. Fu, J. Austin, A. Gettelman, F. Li, and H. Vömel (2008), Observationally derived and general circulation model simulated tropical stratospheric upward mass fluxes, *J. Geophys. Res.*, **113**, D00B07, doi:10.1029/2008JD009945.